Alpha1 and Beta3 Adrenergic Receptor-Mediated Mesolimbic Homeostatic Plasticity Confers Resilience to Social Stress in Susceptible Mice

Supplemental Information

Animals

Male seven-week-old C57BL/6J (Jackson Laboratory) and CD1 retired breeders (Charles River) were purchased and used to set up the chronic social defeat stress paradigm. Ten-week-old DAT-IRES-Cre knock-in mice (1) were used to determine the gene expression of adrenoceptors in projection-specific VTA dopamine (DA) neurons with circuit-mapping molecular profiling technique Retro-TRAP (2, 3). All mice were singly housed on a 12 h light-dark schedule with food and water available *ad libitum*. All experiments performed were approved by the Icahn School of Medicine at Mount Sinai, Institutional Animal Care and Use Committee, and were in accordance with the National Institutes of Health guidelines.

Chronic social defeat stress (CSDS) paradigm

CSDS was performed according to published protocols (4-9). Briefly, CD-1 aggressor mice were housed in their home cages on one side of a clear, perforated plexiglass divider 24 h before the start of social defeat. Each day, after 10 minutes of physical interaction, the aggressor and experimental C57BL/6J mouse maintained sensory contact for 24 h using the perforated plexiglass partition, dividing the resident home cage in two. The experimental mice were exposed to a new CD1 mouse each day for

10 consecutive days. On the tenth day after social defeat, experimental mice were singly housed.

Social interaction test

Social interaction tests were performed on day 11 or after related pharmacological and optogenetic treatments performed in the study. We measured the time spent in the interaction zone, corner zones and locomotor activity during the first (CD1 target absent) and second (CD1 target present) trials in an open-field arena. Their movements were monitored and recorded (Ethovision 10.0, Noldus Information Technology) for 2.5 minutes each test session. The segregation of susceptible and resilient mice was based on the social interaction ratio, which was calculated as [100 × (interaction time, target present)/(interaction time, target absent)] as described previously (4-8). Interaction zone time, corner zone time, total distance travelled and velocity were collected and analyzed. All mice with a ratio above 100 were classified as resilient, and all mice with a ratio below 100 were classified as susceptible.

Sucrose preference test

The sucrose preference test was performed as we previously reported (7). Briefly, mice were initially habituated to two 50-ml tubes filled with drinking water 2 days before the sucrose-preference measurements. After completion of the social-interaction test, mice were given access to a two-bottle choice of water or 1% sucrose solution. Bottles containing water and sucrose were weighed at several time points (12 h, 24 h, 72 h). The position of the bottles was interchanged (left to right,

right to left) after each weight measurement to ensure that the mice did not develop a side preference. Sucrose preference was calculated as a percentage (amount of sucrose consumed/total volume consumed). Total sucrose consumption during the first 24 h after the social-interaction test was measured and used to obtain sucrose preference in this study.

Forced swim test

The FST was performed as previously described (8). Mice were placed for 6 min in a 4 L Pyrex glass beaker containing 3 L of water at 24 ± 1°C. The water was changed between test subjects. All test sessions were recorded by Ethovision software, a digital tracking program. Time spent immobile was independently analyzed by Ethovision 10.0 software (Noldus Information Technology). Increased immobility time and decreased latency to immobility were used as measures of behavioral despair.

***Ex vivo* electrophysiology**

Mice were anaesthetized with isoflurane and perfused immediately with ice-cold aCSF (artificial cerebrospinal fluid), which contained (in mM): 128 NaCl, 3 KCl, 1.25 NaH_2PO_4, 10 D-glucose, 24 $NaHCO_3$, 2 $CaCl_2$ and 2 $MgCl_2$ (oxygenated with 95% O_2 and 5% CO_2, pH 7.4, 295–305 mOsm). Acute brain slices containing LC or VTA were cut using a microslicing vibratome (DTK-1000, Ted Pella) in ice-cold sucrose aCSF, which was derived by fully replacing NaCl with 254 mM sucrose and saturated by 95% O_2 and 5% CO_2. Slices were maintained in holding chambers with aCSF for 1 h recovery at 37°C. For measurements of the spontaneous activity of putative VTA DA

neurons, cell-attached recordings were performed in acutely prepared VTA-containing brain slices obtained from Lumafluor-injected mice. Whole-cell recordings were performed in Lumafluor-labeled VTA→NAc projecting neurons for I_h and K^+ current measurements. I_h currents were recorded with series of 3 s pulses with 10 mV command voltage steps from -120 mV to -60 mV from a holding potential at -60 mV. K^+ currents were recorded with series of 4 s pulses with 10 mV step voltage from -60 mV to 30 mV at a holding potential of -60 mV in the presence of aCSF containing 1 µM tetrodotoxin, 200 µM $CdCl_2$, 1 mM kynurenic acid and 100 µM picrotoxin (8). For validation of optical stimulation, whole-cell current- and voltage-clamp recordings were obtained from putative LC NE neurons in acute LC brain slices cut from C57BL/6J mice that were stereotaxically injected with AAV5-EF1a-DIO-ChR2(H134R)-eYFP into the LC and AAV2/5-AMV-HI-Cre-WPRE-SV40 into the VTA. Patch pipettes (6-8 MΩ for VTA cell-attached recordings, and 2.5-3.5 MΩ for whole-cell recordings) were filled with internal solution containing the following (mM): 115 potassium gluconate, 20 KCl, 1.5 $MgCl_2$, 10 phosphocreatine, 10 HEPES, 2 magnesium ATP and 0.5 GTP (pH 7.2, 285 mOsm). Series resistance was monitored during the experiments and membrane currents and voltages were filtered at 3 kHz (Bessel filter). Data acquisition was collected using a Digidata 1440A digitizer and pClamp 10.2 (Axon Instruments).

In vivo single-unit electrophysiological recording

As we previously reported, mice were anesthetized with 10% chloral hydrate (400 mg/Kg), and head fixed onto a stereotaxic frame horizontally (4). Using bregma, LC was located within the range (in mm): anterior/posterior: -5.30 to -5.50, medial/lateral: 0.50 to 1.20, dorsal/ventral: -2.70 to -4.00. Glass micropipettes (15-20 MΩ) filled with 2 M NaCl were used for recording. Putative LC neurons were identified with the following criteria: spontaneous activity displaying a regular rhythm and firing rates between 0.5 and 5.0 Hz, typical positive-negative long-lasting action potential (>2 ms), biphasic post-excitation inhibition response to contralateral paw pinch (10, 11). Burst firing of LC neurons was determined by a train of at least two spikes with the first interval <80 ms and termination interval >160 ms, as previously reported (12, 13). Using a DP-311 Differential Amplifier (Warner Instruments), electrical signals were amplified and filtered (0.3 -1 kHz). Spontaneous firing rates, burst firing frequencies, percentage of bursting time and bursting spikes, and spike numbers per burst were collected and analyzed. *In vivo* firing activity was analyzed with MATLAB.

Stereotaxic surgeries and microinjections

Mice were anaesthetized with a ketamine (100 mg/kg) and xylazine (10 mg /kg) mixture, placed in a stereotaxic apparatus (Kopf Instruments) and their skull was exposed by scalpel incision. For virus or Lumafluor injections, 33-gauge needles were placed bilaterally at a 7° angle into the VTA (in mm): anterior/posterior, –3.3; lateral/medial, +0.5; dorsal/ventral, –4.6, at a 10° angle into the NAc (in mm):

anterior/posterior, +1.6 ; lateral/medial, +1.5 ; dorsal/ventral, –4.4 (7-9), or at a 0° angle into the LC (in mm): anterior/posterior, –5.45; lateral/medial, +1.28; dorsal/ventral, –3.65 (14), and a volume of 0.5 µl was injected into each hemisphere at a rate of 0.1 µl/min. Needles were slowly removed 5 min after injection to prevent backflow. For chemical injections, bilateral cannulae (26-gauge), with a length of 4.0 mm from the cannula base, were implanted over the VTA (in mm): anterior/posterior, –3.3; lateral/medial, +0.5; dorsal/ventral, –3.7.

Mice were allowed to recover for at least 5 days before starting the following procedures. A cocktail of α1 and β3 receptor agonists (methoxamine hydrochloride 0.02 µg + CL316243 0.6 µg in 0.4 µl of PBS) or PBS-vehicle was infused bilaterally once a day for 10 days for social interaction test and in vitro slice recordings. Injector cannula was removed 5 min after the stopping of each injection to prevent backflow. A cocktail of α1 and β3 receptor antagonists (cyclazosin hydrochloride 0.2 µg + SR59230A 0.02 µg in 0.4 µl of PBS) or PBS vehicle was infused into the VTA 10 minutes before optical stimulation in the LC. Methoxamine hydrochloride, CL316243 and cydazosin were purchased from Sigma; SR59230A was purchased from TOCRIS. Retrograde AAV2/5-AMV-HI-Cre-WPRE-SV40 was purchased from the University of Penn Vector Core, AAV5-EF1a-DIO-ChR2(H134R)-eYFP was purchased from the University of North Carolina Vector Core facility (UNC), CAV-GFP from Biocampus Montpellier, and AAV-IV-NBL10 from the Rockfeller University. Green and red Lumafluors were purchased from Lumafluor, Inc.

Ferrule implantation and optical stimulation

Bilateral ferrules were implanted over the LC (in mm): anterior/posterior, –5.45; lateral/medial, +1.00; dorsal/ventral, –3.00 (14). For secure fixture of the implantable cannulae or ferrule to the skull, the skull was dried and industrial-strength dental cement (Grip cement; Dentsply) was added between the base of the implantable fiber and the skull. Optical ferrules (Thor Labs, BFL37-200) were connected using an FC/PC adaptor to a 473 nm blue laser diode (Crystal Laser, BCL-473-050-M), and a stimulator (Agilent Technologies, no. 33220A) was used to generate blue light pulses. For *in vitro* slice electrophysiological validation of ChR2 activation, we tested a 10 Hz, 5 pulse (at a 10 ms width, every 20 s) phasic optical stimulation protocol (14). For acute optical stimulation during social interaction behavior test, we used this pattern during the 2.5 min SI test without social target +2.5 min SI test with social target. For the repeated stimulation, we used the same pattern 20 minutes/day for 10 days. All optical stimulation sites were confirmed by immunostaining post-behavioral tests.

Molecular profiling

DAT-IRES-Cre mice were injected in the NAc with 0.5 µl CAV-GFP (in mm): anterior/posterior, +1.35; lateral/medial, ±1.0; dorsal/ventral, ±4.2, as well as in the VTA with 0.5 µl AAV-IV-NBL10 (in mm): anterior/posterior, ±3.15; lateral/medial, ±0.5; dorsal/ventral, ±4.2. After viral injections, the needle was left in place for 5 minutes before slowly retracting. Fifteen days after injections, mice were sacrificed and the VTA was rapidly dissected on ice. Briefly, a 2 mm slice was acquired from the region

2~4 mm posterior to bregma. Lateral and dorsal parts were removed to isolate the ventral midbrain. Brains were then pooled into three groups of six mice per group, homogenized in the presence of recombinant nanobody (100 ng/ml, ChromoTek), and centrifuged to clarify. GFP Immunoprecipitation was performed with two mouse monoclonal antibodies (19C8, 19F7; (15)) according to previous protocols (2, 3). The resulting RNA was purified using the Absolutely RNA Nanoprep Kit (Agilent) and analyzed using an Agilent 2100 Bioanalyzer, followed by reverse transcription (QIAGEN QuantiTect) and Taqman qPCR. Libraries for RNA-seq were prepared with oligo dT priming using the SMARTer Ultra Low RNA Kit (Clontech) and analyzed on an Illumina HiSeq 2500. Gene expression was normalized to large ribosomal protein gene 123(rp123) (2).

Immunohistochemistry

Mice were transcardially perfused with PBS, followed by 4% paraformaldehyde (PFA) under general anesthesia with 15% urethane. Brains were post-fixed overnight at 4°C, and then treated with 30% sucrose at 4°C for 2 days. The brains were sectioned at a thickness of 30 μm. VTA slices were obtained and used to validate the expression of AAV-IV-NBL10 and CAV-GFP in DA neurons with rabbit anti-TH (1:1,000, Pel-Freeze), chicken anti-GFP (1:1,1000, Abcam), and rabbit-HA (1:1000, Cell Signaling, to detect HA-conjugated NBL10) primary antibodies and Alexa Flour-conjugated secondary antibodies (Invitrogen). All images were captured on a Zeiss LSM780 confocal microscope at the Icahn School of Medicine Microscopy Core.

Statistics

Data are presented as mean ± s.e.m. All analyses were performed with Prism software. Normality of the data was statistically tested by the D'Agostino-Pearson omnibus normality test. Normally distributed data from multiple-groups were compared with one-way analysis of variance (ANOVA) with/without repeated factors, followed by a post-hoc Bonferroni's multiple comparison test when appropriate. Data that did not pass the normality test was analyzed using a nonparametric Kruskal-Willis test followed by Dunn's multiple comparisons test. The expression ratios of adrenergic receptor genes were compared with a paired Student's t-test. Statistical significance was set at $P< 0.05$.

Supplementary Figures

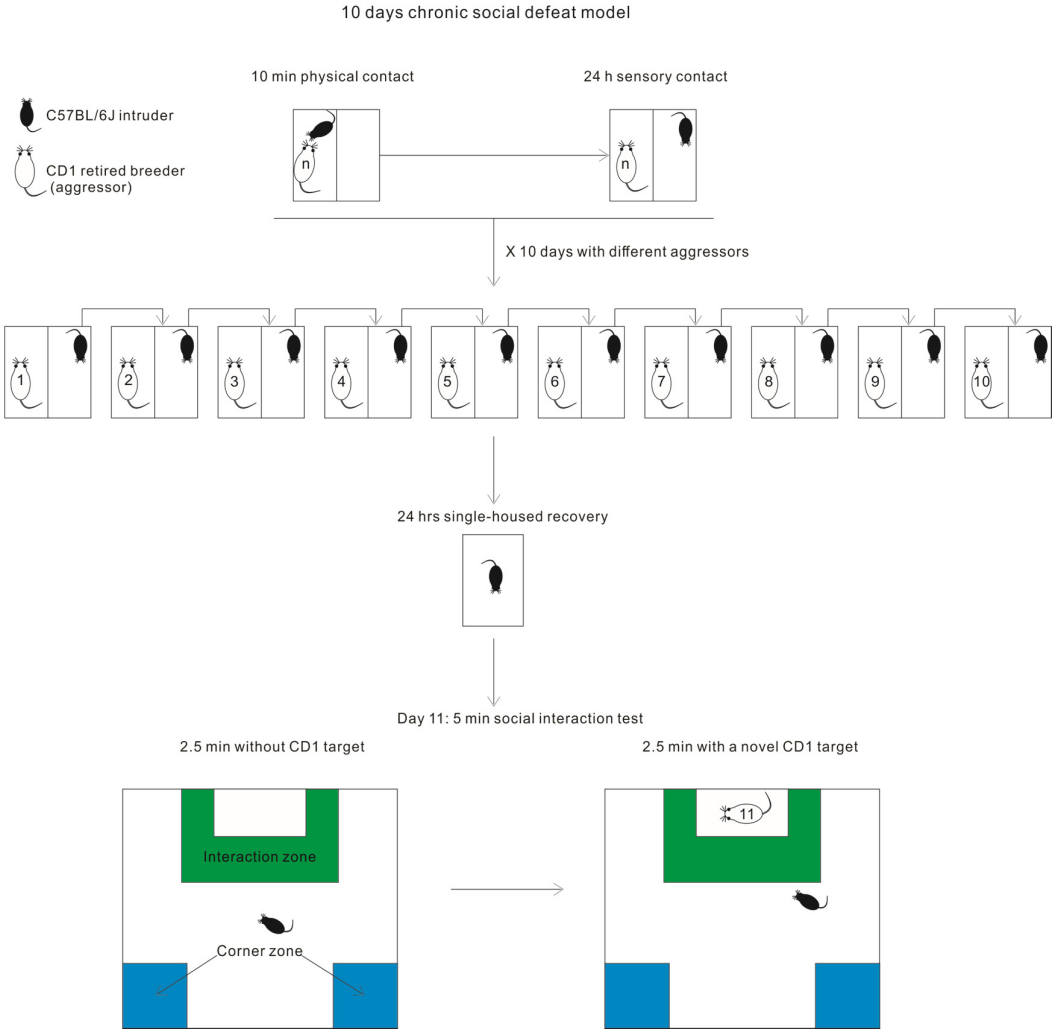

Figure S1. Chronic (10-day) social defeat stress model. Schematic showing 10-day social defeat paradigm using1 C57BL/6J mice and 10 different CD1 retired breeders (aggressor).

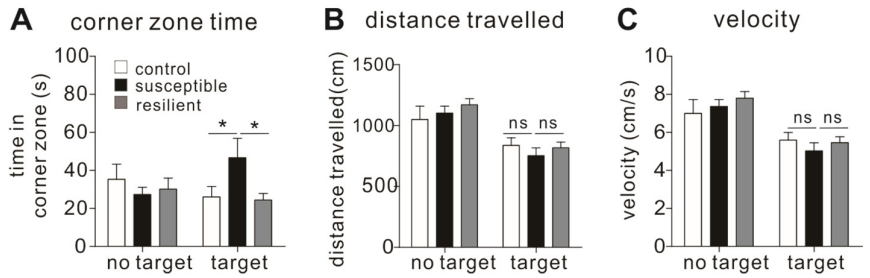

Figure S2. Corner zone time, distance travelled and velocity in social interaction test on day 11. (**A**) Corner zone time (*two-way ANOVA*, $F_{2,52}$=4.015, P=0.0239, *post-hoc Bonferroni's test*: control vs. susceptible, *P=0.0236, susceptible vs. resilient, *P=0.0174, n=9-10 mice/group). (**B**) Distance travelled (*two-way ANOVA*, $F_{2,52}$=0.6888, P=0.5067, n=9-10 mice/group). (**C**) Velocity (*two-way ANOVA*, $F_{2,52}$=0.6888, P=0.5067, n=9-10 mice/group). Error bars indicate mean ±s.e.m. ns, no significance.

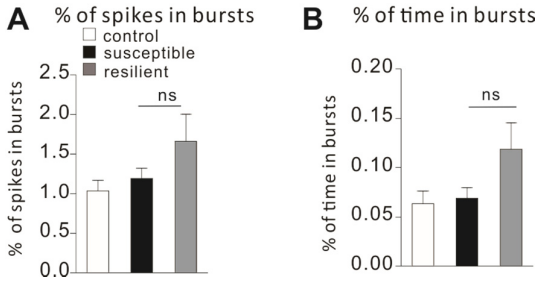

Figure S3. Percentages of spikes in bursts and percentage of time in bursts measured from *in vivo* LC neurons of the three groups. (**A**) Percentage of spikes in bursts (one-*way ANOVA*, $F_{2,80}$=1.646, *P*=0.1993, *post-hoc Bonferroni's test*: control vs susceptible, P>0.9999, susceptible vs. resilient, P=0.0.5001, n=17-34 cells/6-8 mice/group). (**B**) Percentage of time in bursts (one-*way ANOVA*, $F_{2,80}$=2.433, *P*=0.0943, *post-hoc Bonferroni's test*: control vs. susceptible, P>0.9999, susceptible vs. resilient, P=0.1678, n=17-34 cells/6-8 mice/group). Error bars indicate mean ± s.e.m.

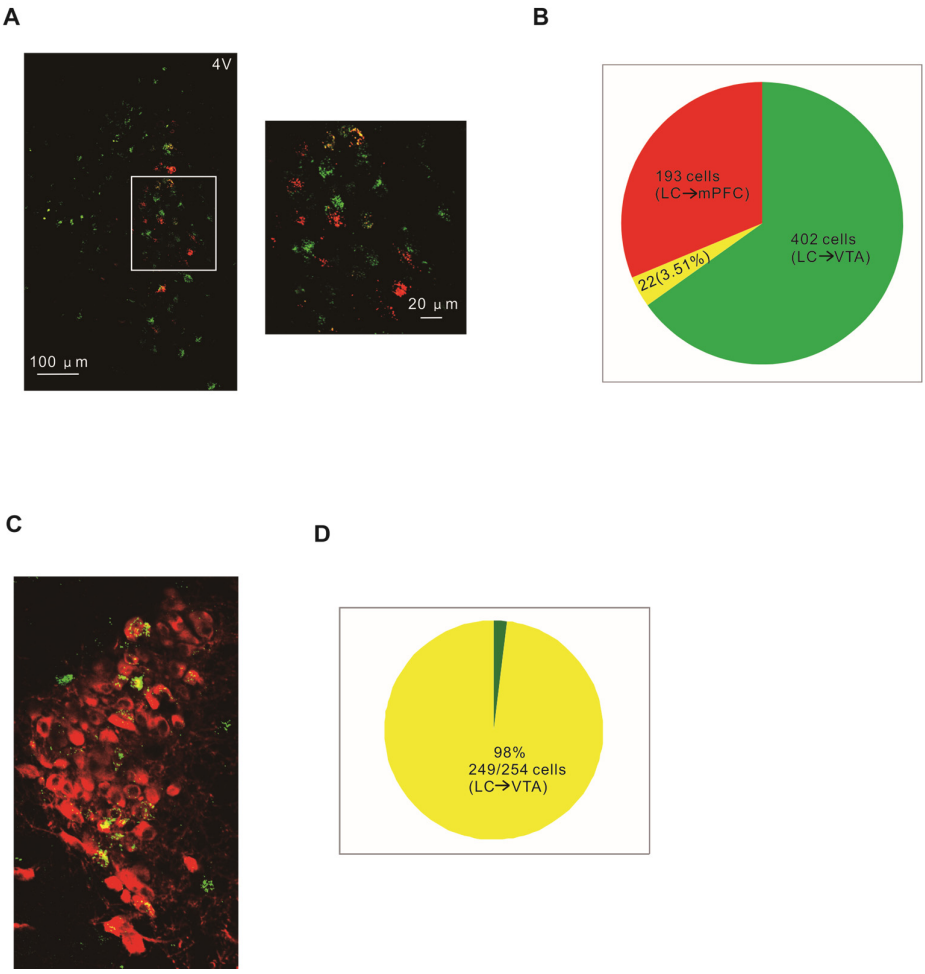

Figure S4. Lumafluor labeling in LC neurons and statistic data. (**A**) Confocal imaging showing lumafluor positive labeling in LC→VTA neurons (Green) and LC→mPFC neurons (Red). (**B**) Number of lumafluor-positive LC→mPFC and LC→VTA neurons, and double labeled neurons. **(C).** Confocal imaging showing green lumafluor-labeled LC→VTA projecting neurons overlapping with TH^+ LC neurons (n=2 mice). **(D).** Percentage of NE neurons in LC→VTA projecting cells (249/254).

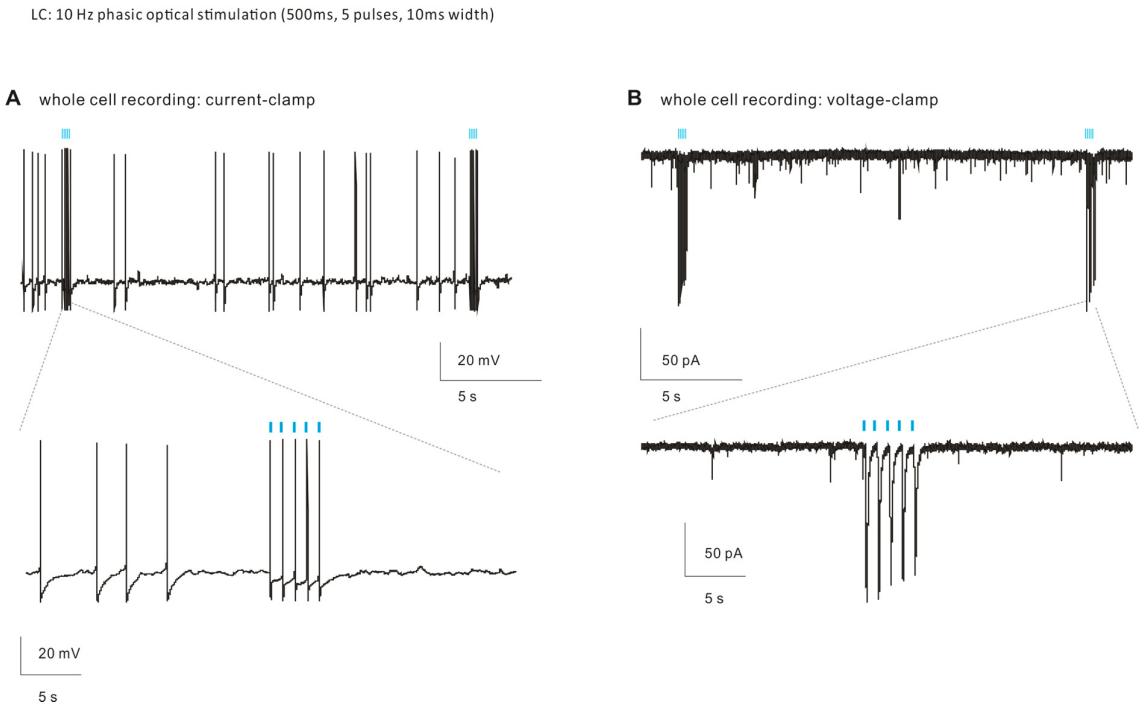

Figure S5. Electrophysiological validation of ChR2 expression in LC→VTA neurons. (**A**) Optical stimulation-induced five spikes obtained under whole-cell current-clamp mode. (**B**) Optical stimulation-induced photocurrent obtained under whole-cell voltage-clamp mode.

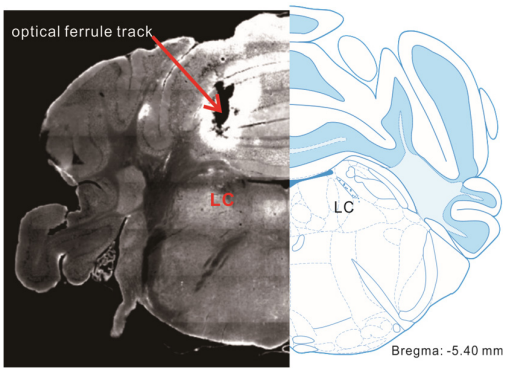

Figure S6. Optical ferrule track and schematic showing LC location.

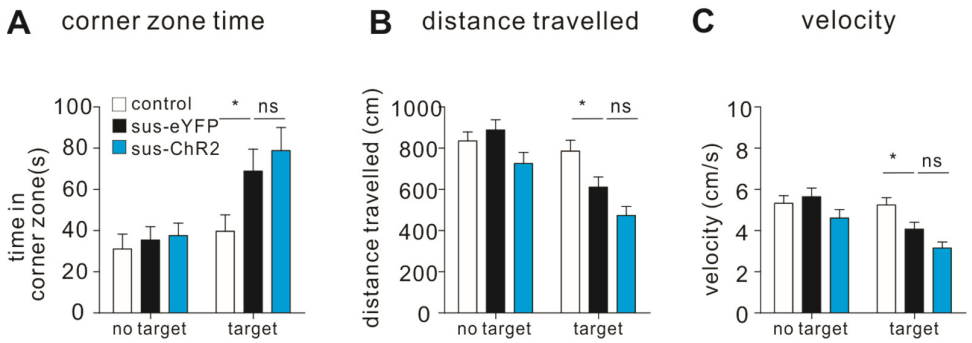

Figure S7. Corner zone time, distance travelled and velocity measured during social interaction test and optical stimulation. (**A**) Corner zone time (*two-way ANOVA*, $F_{2,124}$=2.075, *P*=0.1299, *post-hoc Bonferroni's test*, control vs. sus-eYFP, *P=0.0491, sus-eYFP vs. sus-ChR2, P>0.9999, n=21-23 mice/group). (**B**) Distance traveled (*two-way ANOVA*, $F_{2,124}$=3.811, *P*=0.0248, *post-hoc Bonferroni's test*, control vs. sus-eYFP, *P=0.0314, sus-eYFP vs. sus-ChR2, P=0.1460, n=21-23 mice/group). (**C**) Velocity (*two-way ANOVA*, $F_{2,124}$=3.811, *P*=0.0248, *post-hoc Bonferroni's test*, control vs. sus-eYFP, *P=0.0314, sus-eYFP vs. sus-ChR2, P=0.1460, n=21-23 mice/group). Error bars indicate mean ±s.e.m. ns: no significance.

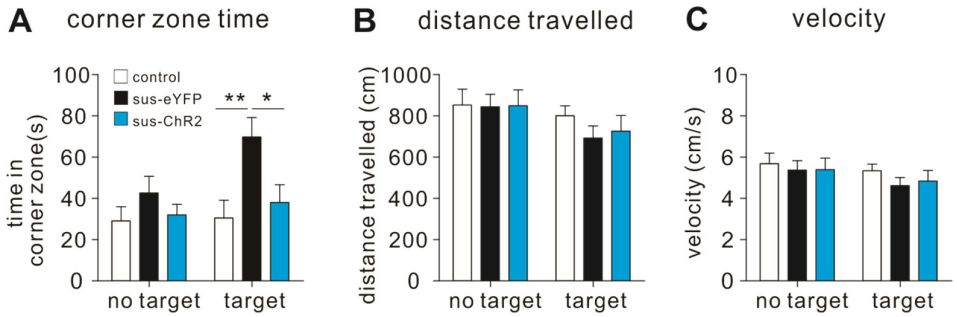

Figure S8. Corner zone time, distance travelled and velocity measured after 5 days of repeated optical stimulation. (**A**) Corner zone time (*two-way ANOVA*, $F_{2,122}$=1.392, *P*=0.2524, *post-hoc Bonferroni's test*, control vs. sus-eYFP, **P=0.0015, sus-eYFP vs. sus-ChR2, *P=0.0237, n=20-23 mice/group). (**B**) Distance travelled (*two-way ANOVA*, $F_{2,122}$=0.4033, *P*=0.669, *post-hoc Bonferroni's test*, sus-eYFP vs. sus-ChR2, P>0.9999, n=20-23 mice/group). (**C**) Velocity (*two-way ANOVA*, $F_{2,122}$=0.4033, *P*=0.669, *post-hoc Bonferroni's test*, sus-eYFP vs. sus-ChR2, P>0.9999, n=20-23 mice/group). Error bars indicate mean ±s.e.m. ns: no significance.

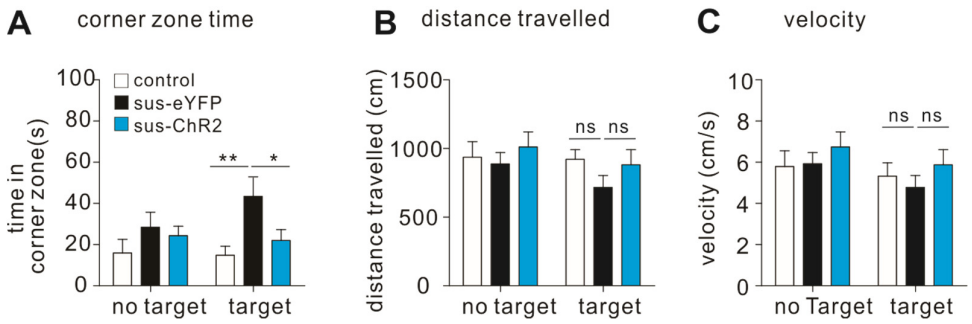

Figure S9. Corner zone time, distance travelled and velocity measured after 10 days of repeated optical stimulation. (**A**) Corner zone time (*two-way ANOVA*, $F_{2,124}$=1.196, *P*=0.3059, *post-hoc Bonferroni's test*, control vs. sus-eYFP, **P=0.0043, sus-eYFP vs. sus-ChR2, *P=0.0418, n=21-23 mice/group). (**B**) Distance travelled (*two-way ANOVA*, $F_{2,124}$=0.3997, *P*=0.6863, *post-hoc Bonferroni's test*, sus-eYFP vs. sus-ChR2, P=0.0418, n=21-23 mice/group). (**C**) Velocity (*two-way ANOVA*, $F_{2,124}$=0.3997, *P*=0.6863, *post-hoc Bonferroni's test*, sus-eYFP vs. sus-ChR2, P=0.0418, n=21-23 mice/group). Error bars indicate mean ±s.e.m. ns: no significance.

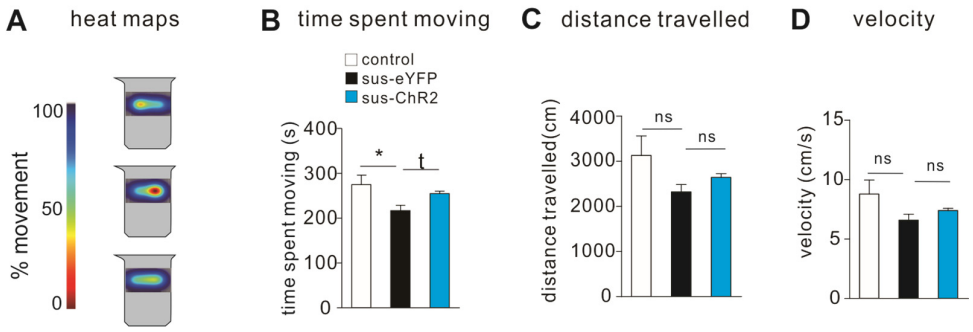

Figure S10. Forced swim test data after 10 days of repeated optical stimulation. (**A**) Sample forced swim test heat maps. (**B**) Time spent moving (*Dunn's multiple comparisons test*: control vs. sus-eYFP, *P=0.0340, sus-eYFP vs. sus-ChR2, ^{t}P=0.0563, n=5-8 mice/group). (**C**) Distance travelled (one-way ANOVA, $F_{2,17}$=3.115, P=0.0704, *post-hoc Bonferroni's test*, control vs. sus-eYFP, P=0.0695, sus-eYFP vs. sus-ChR2, P=0.8229, n=5-8 mice/group). (**D**) Velocity (*one-way ANOVA*, $F_{2,17}$=3.115, P=0.0704, *post-hoc Bonferroni's test*, control vs. sus-eYFP, P=0.0695, sus-eYFP vs. sus-ChR2, P=0.8229, n=5-8 mice/group). Error bars indicate mean ±s.e.m. ns: no significance.

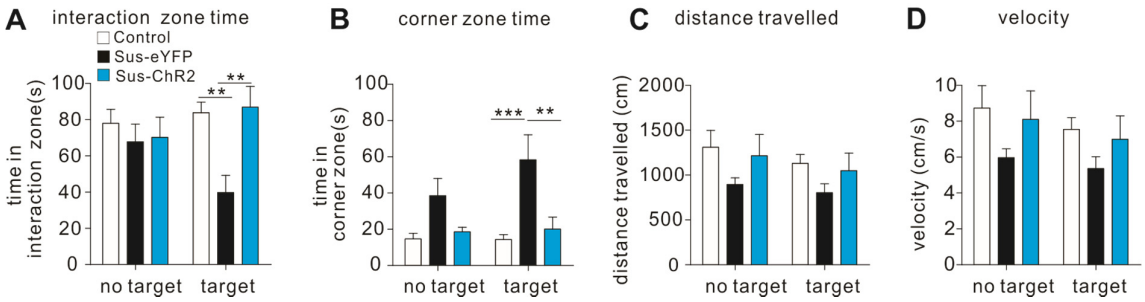

Figure S11. Social interaction behaviors tested after 10 days of repeated optical stimulation of LC→VTA neurons. (**A**) Interaction zone time (*one-way ANOVA*, $F_{2,40}$=3.093, P=0.0527, *post-hoc Bonferroni's test*, control vs. sus-eYFP, **P=0.0026, sus-eYFP vs. sus-ChR2, **P=0.0024, n=10-13 mice/group). (**B**) Corner zone time (*one-way ANOVA*, $F_{2,40}$=2.377, P=0.1015, *post-hoc Bonferroni's test*, control vs. sus-eYFP, ***P<0.0002, sus-eYFP vs. sus-ChR2, **P=0.003, n=10-13 mice/group). (**C**) Distance travelled (*one-way ANOVA*, $F_{2,40}$=0.04378, P=0.9572, *post-hoc Bonferroni's test*, control vs. sus-eYFP, P=0.4387, sus-eYFP vs. sus-ChR2, P=0.9144, n=10-13 mice/group). (**D**) Velocity (*one-way ANOVA*, $F_{2,40}$=0.04378, P=0.9572, *post-hoc Bonferroni's test*, control vs. sus-eYFP, P=0.4387, sus-eYFP vs. sus-ChR2, P=0.9144, n=10-13 mice/group). Error bars indicate mean ±s.e.m.

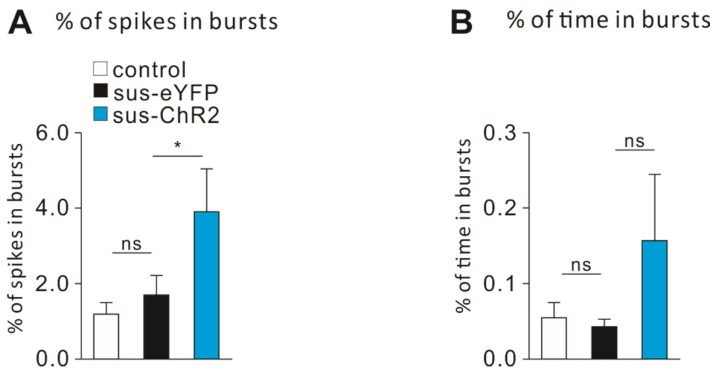

Figure S12. Percentage of spikes in bursts and percentage of time in bursts after 10 days repeated optical stimulation in LC→VTA projecting neurons. (**A**) Percentage of spikes in bursts (*one-way ANOVA*, $F_{2,40}$=6.051, P=0.0051, *post-hoc Bonferroni's test*, sus-eYFP vs. sus-ChR2, *P=0.0447, n=9-20 cells/4-7 mice/group). (**B**) Percentage of time in bursts (*one-way ANOVA*, $F_{2,40}$=1.315, P=0.2798, *post-hoc Bonferroni's test*, sus-eYFP vs. sus-ChR2, P=0.5784, n=9-20 cells/4-7 mice/group). Error bars indicate mean ±s.e.m. ns: no significance.

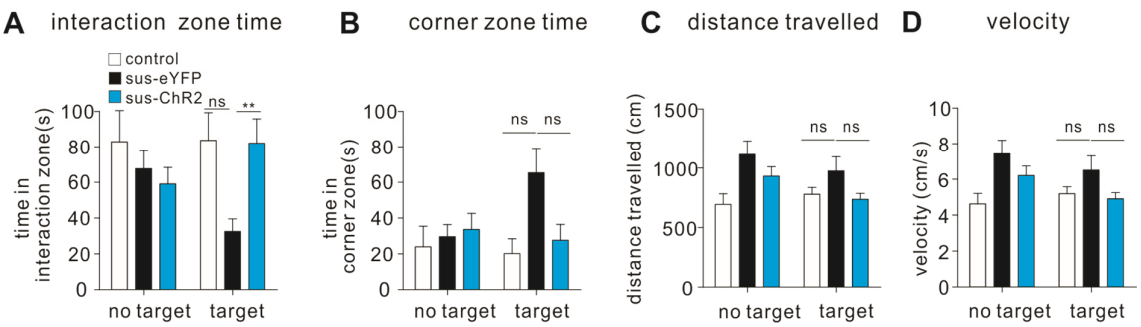

Figure S13. Social interaction behaviors tested after 10 days of repeated optical stimulation of LC→VTA neurons. (**A**) Interaction zone time (*two-way ANOVA*, $F_{2,36}$=2.822, P=0.0727, *post-hoc Bonferroni's test*: control vs. sus-eYFP, P=0.0573; sus-eYFP vs. sus-ChR2, *P=0.0429, n=6-8 mice/group). (**B**) Corner zone time (*two-way ANOVA*, $F_{2,36}$=2.194, P=0.1262, *post-hoc Bonferroni's test*: control vs. sus-eYFP, P=0.347; sus-eYFP vs. sus-ChR2, P=0.1569, n=6-8 mice/group). (**C**) Distance travelled (*two-way ANOVA*, $F_{2,36}$=1.369, P=0.2847, *post-hoc Bonferroni's test*: control vs. sus-eYFP, P=0.4235; sus-eYFP vs. sus-ChR2, P=0.1707, n=6-8 mice/group). (**D**) Velocity (*two-way ANOVA*, $F_{2,36}$=1.369, P=0.2847, *post-hoc Bonferroni's test*: control vs. sus-eYFP, P=0.4235; sus-eYFP vs. sus-ChR2, P=0.1707, n=6-8 mice/group). Error bars indicate mean ±s.e.m.

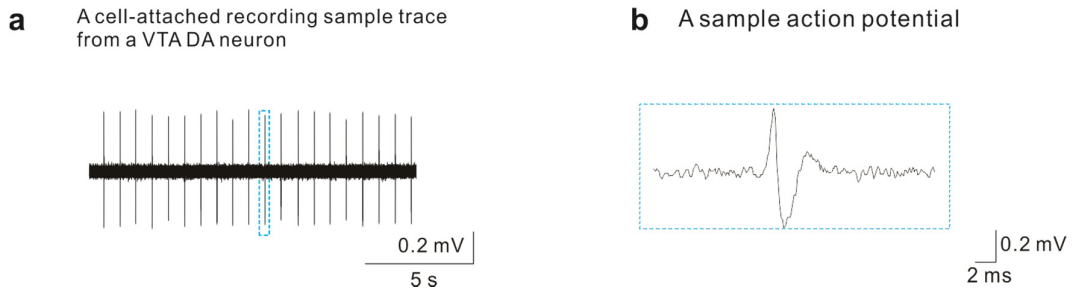

Figure S14. Sample traces recorded from VTA→NAc neurons. (**A**) A cell-attached recording sample trace from a VTA-NAc neuron. (**B**) An action potential sample trace.

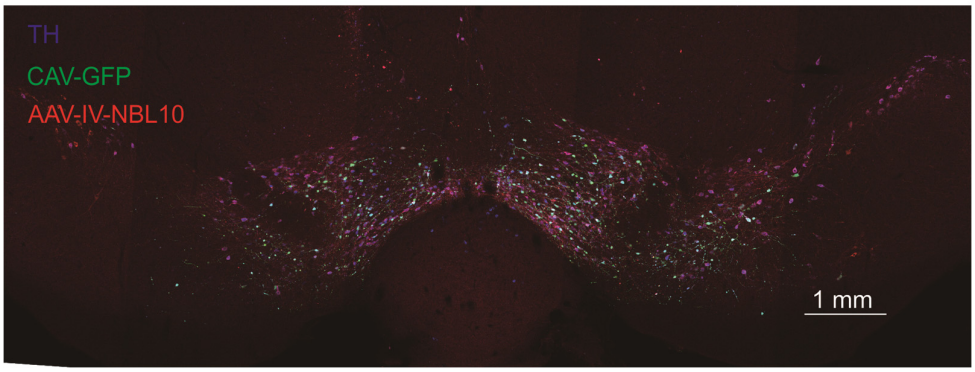

Figure S15. Confocal imaging showing expression of GFP and NBL10 in VTA→DA neurons. This is a representative image showing GFP (green) and NBL10 (red) expression in TH-positive neurons (blue) neurons from one mouse.

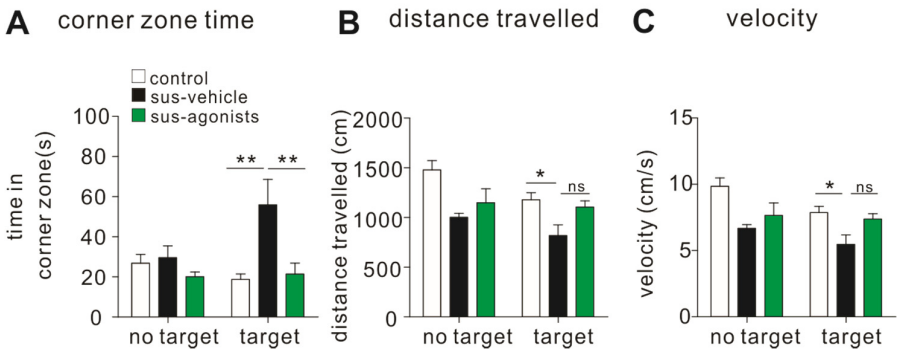

Figure S16. Corner zone time, distance travelled and velocity measured after 10 days of intra-VTA infusion of α1 and β3 adrenoceptor agonists. (**A**) Corner zone time (*two-way ANOVA*, $F_{2,54}$=4.245, P=0.0194, *post-hoc Bonferroni's test*: control vs. sus-vehicle, **P=0.003; sus-vehicle vs. sus-agonists, **P=0.0022, n=9-12 mice/group). (**B**) Distance travelled (*two-way ANOVA*, $F_{2,54}$=1.042, P=0.3579, *post-hoc Bonferroni's test*: control vs. sus-vehicle, *P=0.0181; sus-vehicle vs. sus-agonists, P=0.1133, n=9-12 mice/group). (**C**) Velocity (*two-way ANOVA*, $F_{2,54}$=1.042, P=0.3579, *post-hoc Bonferroni's test*: control vs. sus-vehicle, *P=0.0181; sus-vehicle vs. sus-agonists, P=0.1133, n=9-12 mice/group). Error bars indicate mean ±s.e.m.

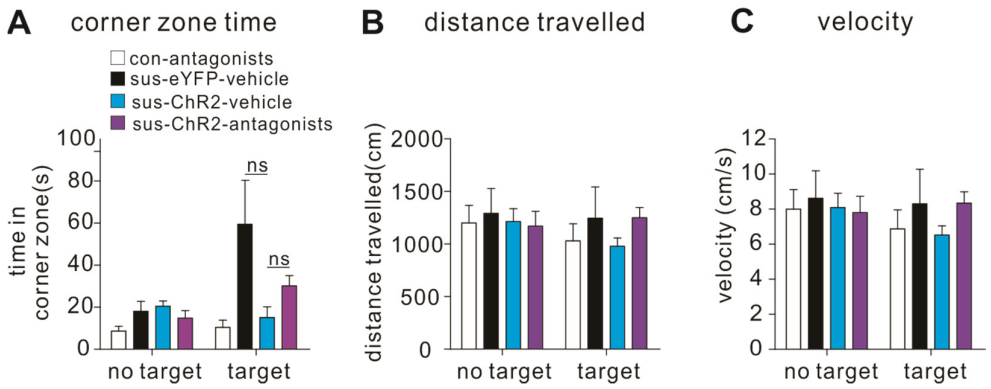

Figure S17. Corner zone time, distance travelled and velocity measured after 10 days repeated optical stimulation and intra-VTA infusion of α1 and β3 adrenoceptor antagonists. (**A**) Corner zone time (*two-way ANOVA*, $F_{3,42}$=2.608, P=0.064, *post-hoc Bonferroni's test*: sus-eYFP-vehicle vs. sus-ChR2-vehicle, P=0.0709; sus-ChR2-vehicle vs. sus-ChR2-antagonists, P>0.999, n=5-7 mice/group). (**B**) Distance travelled (*two-way ANOVA*, $F_{3,42}$=2.608, P=0.064, *post-hoc Bonferroni's test*: sus-eYFP-vehicle vs. sus-ChR2-vehicle, P>0.999; sus-ChR2-vehicle vs. sus-ChR2-antagonists, P=0.1188, n=5-7 mice/group). (**C**) Velocity (*two-way ANOVA*, $F_{3,42=2.608}$, P=0.064, *post-hoc Bonferroni's test*: sus-eYFP-vehicle vs. sus-ChR2-vehicle, P>0.999; sus-ChR2-vehicle vs. sus-ChR2-antagonists, P=0.1188, n=5-7 mice/group). Error bars indicate mean ±s.e.m.

Supplemental References

1. Rothbauer U, Zolghadr K, Tillib S, Nowak D, Schermelleh L, Gahl A, et al. (2006): Targeting and tracing antigens in live cells with fluorescent nanobodies. *Nat Methods*. 3:887-889.

2. Ekstrand MI, Nectow AR, Knight ZA, Latcha KN, Pomeranz LE, Friedman JM (2014): Molecular profiling of neurons based on connectivity. *Cell*. 157:1230-1242.

3. Nectow AR, Ekstrand MI, Friedman JM (2015): Molecular characterization of neuronal cell types based on patterns of projection with Retro-TRAP. *Nat Protoc*. 10:1319-1327.

4. Cao JL, Covington HE, 3rd, Friedman AK, Wilkinson MB, Walsh JJ, Cooper DC, et al. (2010): Mesolimbic dopamine neurons in the brain reward circuit mediate susceptibility to social defeat and antidepressant action. *The Journal of neuroscience : the official journal of the Society for Neuroscience*. 30:16453-16458.

5. Berton O, McClung CA, Dileone RJ, Krishnan V, Renthal W, Russo SJ, et al. (2006): Essential role of BDNF in the mesolimbic dopamine pathway in social defeat stress. *Science (New York, NY)*. 311:864-868.

6. Krishnan V, Han MH, Graham DL, Berton O, Renthal W, Russo SJ, et al. (2007): Molecular adaptations underlying susceptibility and resistance to social defeat in brain reward regions. *Cell*. 131:391-404.

7. Chaudhury D, Walsh JJ, Friedman AK, Juarez B, Ku SM, Koo JW, et al. (2013): Rapid regulation of depression-related behaviours by control of midbrain dopamine neurons. *Nature*. 493:532-536.

8. Friedman AK, Walsh JJ, Juarez B, Ku SM, Chaudhury D, Wang J, et al. (2014): Enhancing depression mechanisms in midbrain dopamine neurons achieves homeostatic resilience. *Science (New York, NY)*. 344:313-319.

9. Walsh JJ, Friedman AK, Sun H, Heller EA, Ku SM, Juarez B, et al. (2014): Stress and CRF gate neural activation of BDNF in the mesolimbic reward pathway. *Nature neuroscience*. 17:27-29.

10. Torrecilla M, Fernandez-Aedo I, Arrue A, Zumarraga M, Ugedo L (2013): Role of GIRK channels on the noradrenergic transmission in vivo: an electrophysiological and neurochemical study on GIRK2 mutant mice. *Int J Neuropsychopharmacol*. 16:1093-1104.

11. Gobbi G, Cassano T, Radja F, Morgese MG, Cuomo V, Santarelli L, et al. (2007): Neurokinin 1 receptor antagonism requires norepinephrine to increase serotonin function. *Eur Neuropsychopharmacol*. 17:328-338.

12. Miguelez C, Grandoso L, Ugedo L (2011): Locus coeruleus and dorsal raphe neuron activity and response to acute antidepressant administration in a rat model of Parkinson's disease. *Int J Neuropsychopharmacol*. 14:187-200.

13. Miguelez C, Aristieta A, Cenci MA, Ugedo L (2011): The locus coeruleus is directly implicated in L-DOPA-induced dyskinesia in parkinsonian rats: an electrophysiological and behavioural study. *PLoS One*. 6:9.

14. Carter ME, Yizhar O, Chikahisa S, Nguyen H, Adamantidis A, Nishino S, et al. (2010): Tuning arousal with optogenetic modulation of locus coeruleus neurons. *Nature neuroscience*. 13:1526-1533.

15. Doyle JP, Dougherty JD, Heiman M, Schmidt EF, Stevens TR, Ma G, et al. (2008): Application of a translational profiling approach for the comparative analysis of CNS cell types. *Cell*. 135:749-762.